Investigation of Rectenna Array Configurations for Enhanced RF Power Harvesting

Ugur Olgun, *Student Member, IEEE*, Chi-Chih Chen, *Senior Member, IEEE*, and John L. Volakis, *Fellow, IEEE*

***Abstract*—RF power harvesting enables controllable and simultaneous wireless power delivery to many RF devices. Devices built with this unique technology can be sealed, embedded within structures, or made mobile, thus eliminating additional service for a battery. A key component of this technology is the "rectenna," which is composed of antennas and rectifying circuitry to convert RF energy into dc power. Typically, multiple rectenna elements are used to generate the dc power for reliable device operation. This letter compares two different rectenna architectures for maximum RF-to-dc power conversion efficiency. A simple rectenna design example containing a 2×2 planar antenna array will be presented to demonstrate such RF power harvesting technology. The parameter, Rectenna Topology Indicator (RTI), is introduced for performance comparison.**

***Index Terms*—Array configuration, power harvesting, rectenna array, RF power transmission, RFID, zero-bias diode.**

I. Introduction

RECENT advances in semiconductor technology and the introduction of passive RFIDs provided impetus for power harvesting from radio waves [1]. Already, cell phone companies are developing mobile devices charged by harvesting ambient RF power [2]. Likewise, defense companies have been working on systems to power unmanned aerial vehicles (UAVs) while in air by exploiting directed energy from microwave sources [3].

Typically, a single rectenna is not sufficient in supplying energy for reliable device operation. Alternatively, properly interconnecting several antennas could provide for sufficient rectification. In one configuration, multiple antennas can be arranged to channel the RF power to a single rectifier [4] [see Fig. 1(a)]. In a point-to-point RF system (narrow beam), this configuration offers the most efficient power transfer scheme. In another approach, each antenna can incorporate its own rectifier to separately harvest dc power [5] [see Fig. 1(b)]. The harvested dc power from all rectifiers can then be combined in parallel, series, or a hybrid manner [6]. This configuration is suitable when dealing with large rectenna arrays (avoids complex feeds) or harvesting ambient RF power (eliminates random polarization effects). However, in the case of batteryless RFIDs (conventional RFID + sensing, tracking, etc.), the issues are different as the transmitted energy is controlled and a broader reception is necessary. Therefore, an analytical method to evaluate the RF power-harvesting scheme subject to predefined conditions is essential.

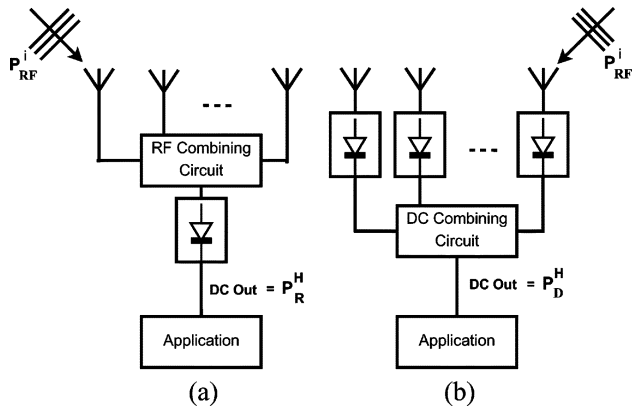

Fig. 1. Schematics of the investigated rectenna array configurations. $P^i_{\rm RF}$ is the incident RF power impinging on the antennas, $P^H_{\rm R}$ refers to the harvested dc power by RF-combiner topology and $P^H_{\rm D}$ denotes the harvested dc power by DC-combiner topology. (a) RF-combiner. (b) DC-combiner.

In this letter, we discuss the advantages and disadvantages of the two RF power-harvesting configurations as shown in Fig. 1. First, we present an analytical approach that can evaluate the power-harvesting performance of the given rectenna topologies. Then, we consider an efficient rectification method using a miniaturized rectenna to better utilize the available aperture. Measurements are presented to evaluate the rectenna's performance and are compared to analytical predictions (for a 2×2 antenna array).

II. Analytical Approach

RF-to-dc conversion efficiency, η, is of paramount importance for optimal wireless power transmission. Consequently, we begin by defining the conversion efficiency as

$$\eta = \frac{\text{Harvested dc Power}}{\text{Input RF Power to Rectifier}} = \frac{P_{\rm DC}}{P_{\rm RF}}. \tag{1}$$

The nonlinear nature of diodes complicates the evaluation of η via analytical means. Specifically, for most rectifier circuits, η changes with RF input power, operating frequency, impedance matching, and diode properties (i.e., breakdown voltage, diode parasitics, etc.). In this letter, the operating frequency is assured constant, and the diodes are chosen to be identical, viz. $\eta = \eta(P_{\rm RF})$. Also, good models to estimate η can be found in literature [7] and are used herewith

$$\eta = \frac{V_{\rm D} I_{\rm out}}{\frac{1}{T}\int_0^T v_{\rm in}(t) i_{\rm D}(t) dt}. \tag{2}$$

Manuscript received December 19, 2010; revised February 18, 2011; accepted March 23, 2011. Date of publication April 05, 2011; date of current version April 14, 2011.

The authors are with the ElectroScience Laboratory, Electrical and Computer Engineering Department, The Ohio State University, Columbus, OH 43212 USA (e-mail: olgunu@ece.osu.edu).

Color versions of one or more of the figures in this letter are available online at http://ieeexplore.ieee.org.

Digital Object Identifier 10.1109/LAWP.2011.2136371

In this, T is the period of the input RF signal, $v_{\rm in}(t)$ is the input voltage to the rectifier, and $i_{\rm D}(t)$ is the current flowing through the diode terminals. Also, $V_{\rm D}$ denotes the dc voltage on the dc load, and $I_{\rm out}$ is the current flowing through the load terminals.

Radio propagation models are also available to estimate the received RF power. Using a modified version of the Friis transmission formula, the incident RF power impinging on the antennas, $P^i_{\rm RF}$, can be expressed as

$$P^i_{\rm RF} = P_{\rm t}G_{\rm t}\left(\frac{\lambda}{4\pi}\right)^2\left(\frac{1}{R}\right)^n e^{-\alpha R}. \tag{3}$$

Here, $P_{\rm t}$ is the input power to the transmitting antenna and $G_{\rm t}$ is the transmit antenna realized gain. Furthermore, α denotes the effective decay coefficient in air ($\alpha = 0.001$), and n is the path loss exponent. Typically, $n = 2$ in free space and takes a value between 3 and 5 in urban environments (line-of-sight propagation).

Having the diode and radio propagation models at hand, the total harvested dc power by the RF-combiner topology in Fig. 1(a) can be written as

$$P^H_{\rm R} = e_{\rm r}P^i_{\rm RF}G_{\rm r}\eta_{\rm r}. \tag{4}$$

In this, η_r is the RF-to-dc conversion efficiency of the RF-combiner, i.e., $\eta_{\rm r} = \eta\left(e_{\rm r}P^i_{\rm RF}G_{\rm r}\right)$. Also, $e_{\rm r}$ denotes the efficiency of the RF combining circuit, and $G_{\rm r}$ refers to the realized gain of the antenna array.

The total harvested dc power by the DC-combiner topology Fig. 1(b) can be calculated from

$$P^H_{\rm D} = e_{\rm d}\sum_{m=1}^{N} P^i_{\rm RF}G_m\eta_d. \tag{5}$$

In this, $\eta_{\rm d}$ refers to the RF-to-dc conversion efficiency of the DC-combiner, i.e., $\eta_{\rm d} = \eta\left(P^i_{\rm RF}G_m\right)$. Furthermore, $e_{\rm d}$ denotes the efficiency of the dc combining circuit, N is the number of antennas in the array, and G_m refers to the realized gain of the mth antenna element. Assuming that the antenna elements are identical, i.e., $G_{\rm a} = G_m, \forall\, m$, (5) becomes

$$P^H_{\rm D} = e_{\rm d}NP^i_{\rm RF}G_{\rm a} \times \eta\left(P^i_{\rm RF}G_{\rm a}\right). \tag{6}$$

Furthermore, assuming that the rectenna topologies under investigation are planar arrays (having $K \times L = N$ elements situated in the xy plane), and no coupling exists among the array elements, $G_{\rm r}$ in (4) can be related to $G_{\rm a}$ in (6) via

$$G_{\rm r} = G_{\rm a}\frac{\sin\left(\frac{K}{2}\psi_x\right)}{\sin\left(\frac{\psi_x}{2}\right)}\frac{\sin\left(\frac{L}{2}\psi_y\right)}{\sin\left(\frac{\psi_y}{2}\right)} \tag{7}$$

where

$$\psi_x = kd_x\sin\theta\cos\phi \quad \psi_y = kd_y\sin\theta\sin\phi. \tag{8}$$

As usual, k is the wavenumber, and $d_{x,y}$ refer to interelement spacing in the x- and y-directions, respectively, and (θ, ϕ) denote the spherical angles of the field incident onto the receiving antenna.

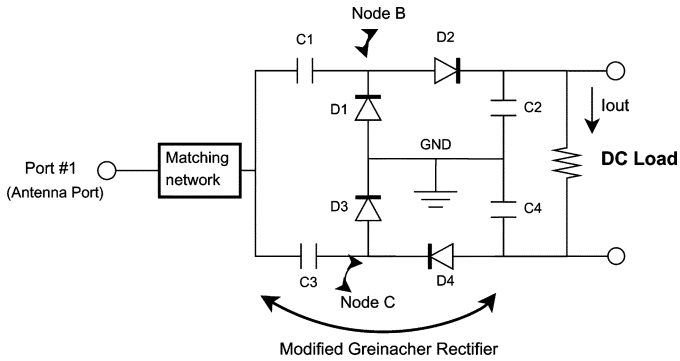

Fig. 2. Schematic of the proposed rectifier. D1–D4 are zero-bias low barrier Schottky diodes (Avago HSMS-2852). These diodes feature high saturation current and do not require additional biasing. C1 = C3 = 100 pF, C2 = C4 = 100 μF, dc load = 10 kΩ.

Substituting (7) into (6), we obtain an expression for the power harvested by the two topologies depicted in Fig. 1. Specifically, we introduce the Rectenna Topology Indicator (RTI) function defined as the ratio of final available dc power from the two topologies. That is, ${\rm RTI} = P^H_{\rm R}/P^H_{\rm D}$. For the above $K \times L$ array, RTI takes the explicit form

$${\rm RTI}(\theta,\phi) = \frac{e_{\rm r}}{e_{\rm d}N}\frac{\sin\left(\frac{K}{2}\psi_x\right)}{\sin\left(\frac{\psi_x}{2}\right)}\frac{\sin\left(\frac{L}{2}\psi_y\right)}{\sin\left(\frac{\psi_y}{2}\right)}\frac{\eta_{\rm r}}{\eta_{\rm d}}. \tag{9}$$

As seen, RTI is a function of the incident angle, $\eta_{\rm r}$ and $\eta_{\rm d}$. Note that $\eta_{\rm r}$ and $\eta_{\rm d}$ must be evaluated for different power levels. As can be surmised, for ${\rm RTI} > 1$, the RF-combiner performs better than the DC-combiner. The converse is true for ${\rm RTI} < 1$. From (9), it can be observed that an increase in N will extend the region where ${\rm RTI} < 1$.

III. Rectenna Design Example

A. Rectifier Design

The efficiency of rectifier design is critical for power harvesting. Toward this goal, we found that a modified version of the single-stage full-wave Greinacher rectifier, depicted in Fig. 2, provides an efficient rectification scheme [7].

The modified Greinacher rectifier operates as follows. If $v_{\rm rec}(t)$ is the induced voltage at the antenna port, then C1 and D1 (Fig. 2) shift the voltage $v_{\rm rec}(t)$ up at node $\boldsymbol{B}$. Subsequently, D2 and C2 rectify the voltage at node $\boldsymbol{B}$ (both RF and dc components) to appear across the dc load. Similarly, C3 and D3 shift the voltage $v_{\rm rec}(t)$ down at node $\boldsymbol{C}$. In turn, D4 and C4 rectify the voltage at node $\boldsymbol{C}$ to appear across the dc load. Upon reaching equilibrium, the rectifier circuit delivers a constant output current and voltage to the dc load.

The impedance matching stage (depicted in Fig. 3) is essential in providing maximum power transfer from the antenna to the rectifier circuit. Designing the matching network is not straightforward since the rectifier is a nonlinear load with complex impedance that varies with frequency and input power level. One design approach is to model the rectifier circuit using experimental characterization at the minimum power level required by the application [8]. This can be done by measuring the input

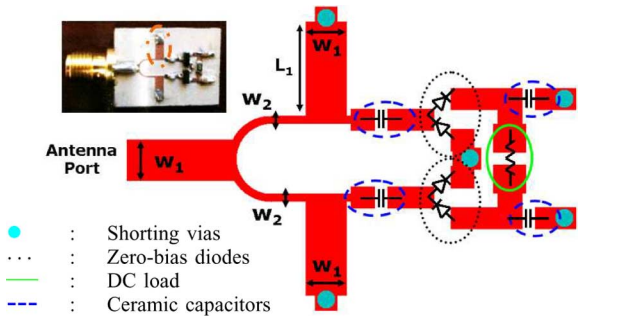

Fig. 3. Layout of the rectifier prototype, printed on RO3206. $w_1 = 72$ mil, $w_2 = 15$ mil, and $L_1 = 171$ mil. Fabricated sample is shown in top left, and the impedance matching stub is encircled.

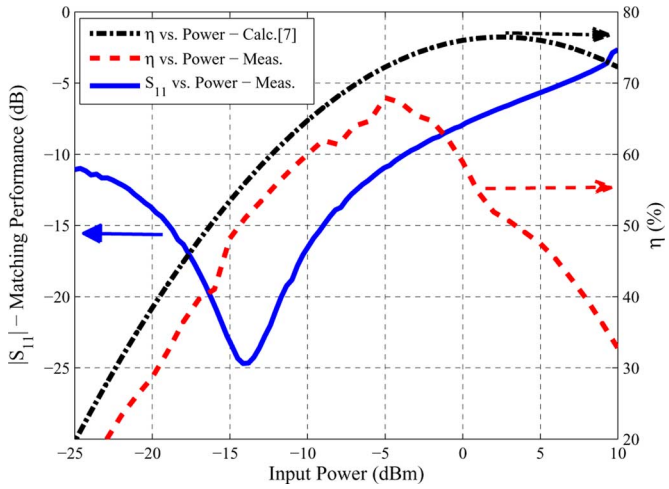

Fig. 4. Measured and calculated η for the presented Greinacher rectifier at 2.45 GHz. Measured $|S_{11}|$ is also given.

impedance (extracted from S_{11}) of the rectifier circuit (with all components) without a matching network at that power level. Using the impedance results from the experimental characterization (i.e., rectifier impedance) and assuming a 50-Ω source load, the matching circuit design is rather straightforward.

Fig. 4 depicts the magnitude of the measured reflection coefficient ($|S_{11}|$) and η of the fabricated prototype as a function of input RF power from -25 to $+10$ dBm. $|S_{11}|$ measurement is conducted by utilizing the power-sweep mode of the network analyzer at 2.45 GHz, and η is calculated by dividing the dc power dissipated on the load by the input RF power. As seen, the rectifier is well matched when the input power is between -25 and -5 dBm. However, the matching network performance deteriorates significantly at higher RF power levels. Also, Fig. 4 shows that the measured η increases monotonically with input power up to -5 dBm. Theoretical predictions (calculated using the model in [7]) are provided as well. We note that deviation of the measured η from theory is due to the deteriorating performance of the impedance matching network (at higher RF power levels) and different than specified parasitic resistance of the diodes (at lower RF power levels).

B. Antenna Design

Critical to the practicality of batteryless RFIDs is the utilization of a small-size antenna with a broad radiation pattern (e.g., microstrip patch) [9]. In this letter, a modified version of the second-iteration Koch fractal geometry (see Fig. 5) was proposed to reduce the patch size. The antenna size was further reduced down to $0.147\lambda_0 \times 0.139\lambda_0$ by employing a high dielectric substrate ($\epsilon_r = 10.2$, thickness $= 50$ mil). Moreover, the Koch patch antenna provides broader radiation pattern compared to a rectangular one [9]. The bandwidth was also improved by employing a capacitively coupled probe feed.

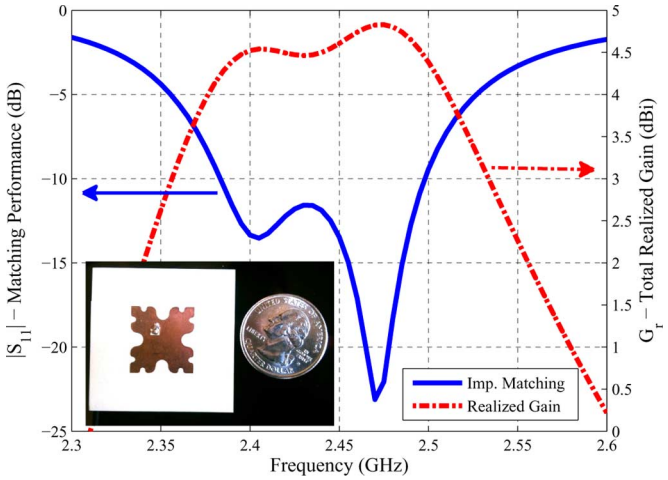

Fig. 5. Measured $|S_{11}|$ performance and total realized gain (at boresight) of the proposed antenna. Fabricated sample is shown in bottom left.

Fig. 5 shows the measured $|S_{11}|$ and realized gain performance of the designed antenna element operating at 2.45 GHz. As seen, the proposed antenna (linearly polarized) has 5% bandwidth (covers the whole ISM band) and greater than 4.5 dBi realized gain at boresight.

IV. Rectenna Array Configurations

Using the designed Koch-type patch antennas, a 2×2 planar array with $\lambda_0/2$ interelement spacing (based on $f_c = 2.45$ GHz) was constructed. This interelement spacing was chosen to combat fading, prevent aliasing, and avoid grating lobes. In addition, the 2×2 array is fabricated such that it can support both of the configurations depicted in Fig. 1.

The power-harvesting capabilities of the 2×2 array were evaluated in the Ohio State University ElectroScience Laboratory, Columbus, with compact range and a controlled environment to minimize multipath effects. For the RF source, a 10-dBi commercial antenna (linearly polarized), transmitting 1 W of continuous-wave (CW) signal at 2.45 GHz, was placed at the line of sight of the aforementioned array. Both antennas were placed 2 m above the ground and 2.5 m away from each other. A four-way RF combiner (MiniCircuits ZB4PD-42+) and four 5-in coaxial cables were utilized to feed the 2×2 array when in RF-combiner configuration. The total insertion loss for the RF combining unit was 1.2 dB, and the efficiency of the dc voltage combining circuit was 90%. We note that, for a fair comparison of the topologies in Fig. 1, dc loads of the rectifiers (depicted in Fig. 2) were optimized separately for each array configuration (face-to-face case only).

To perform the measurements, a computer-controlled multimeter was connected to the rectifier circuit while the 2×2 array

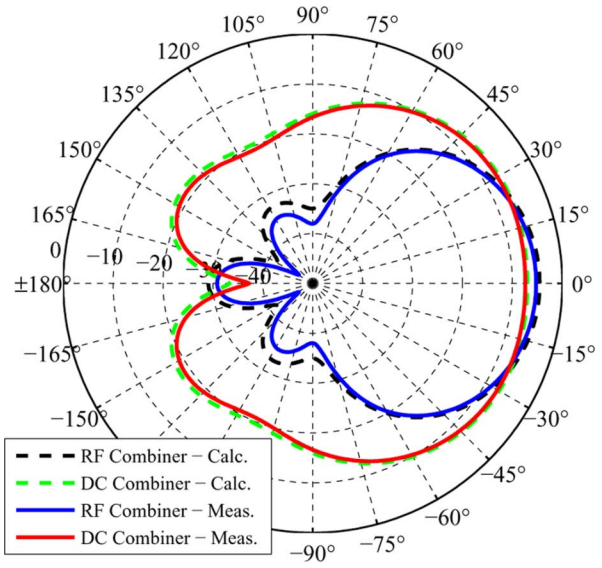

Fig. 6. Measured and calculated dc power (dBm scale) harvested by the two different rectenna topologies. Realized gain of the antennas are simulated by full-wave solvers, and the results are utilized in the calculations.

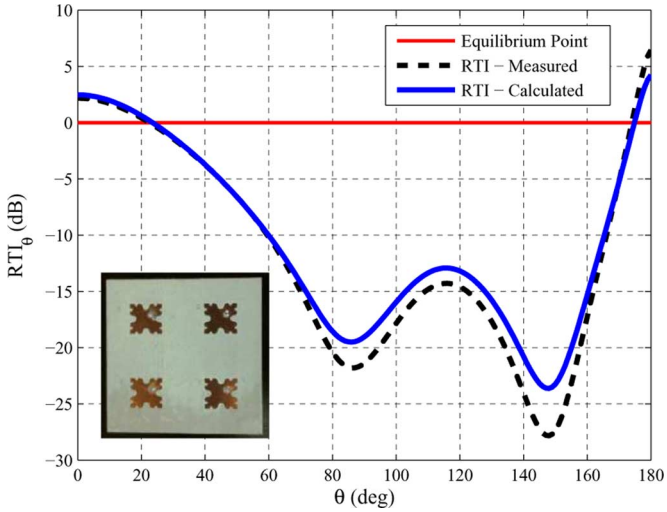

Fig. 7. Measured and calculated RTI versus θ (dB scale). Straight horizontal line depicts the equilibrium line ($P_R^H = P_D^H$). Fabricated sample of the 2×2 array is also shown.

was rotating. The harvested dc voltage (100 measurements at each angle were collected and averaged) was used to calculate the dc power for each configuration. For this particular measurement setup, the RTI simplifies to

$$\mathrm{RTI}(\theta) = \frac{e_\mathrm{r}}{2e_\mathrm{d}} \frac{\sin(\pi \sin\theta)}{\sin\left(\frac{\pi}{2}\sin\theta\right)} \frac{\eta_\mathrm{r}}{\eta_\mathrm{d}}. \tag{10}$$

Fig. 6 compares the measured and calculated harvested dc power from both configurations. Also, Fig. 7 plots the measured and calculated RTI. As seen from Fig. 7, the RF-combiner offers better performance at boresight. However, the DC-combiner configuration performs better as the array is rotating away from normal incidence (greater than $\pm 20°$). This is due to the fact that the individual elements have a broader pattern, whereas for the array, the rectifier observes the narrower beam. Regardless, we remark that our measurements are in good agreement with theoretical predictions.

V. Conclusion

A method for comparing the harvested RF power by the two rectenna topologies in Fig. 1 was presented. This method was validated using a fabricated 2×2 antenna array employing a small size $(0.147\lambda_0 \times 0.139\lambda_0)$ yet efficient (up to 70% conversion efficiency) rectenna elements.

The first topology combined the RF signal from the antenna array to a single rectifier. This topology has the advantage of harvesting more power near the main beam, which is due to the higher power fed to a single rectifier, i.e., utilizing the diodes more efficiently. The other topology rectified the received RF signal of each antenna element prior to combining it at the dc output. This topology can harvest more power at angles away from broadside as each rectifier is connected to the individual antenna elements and responds to the broad pattern of that element. Thus, it is less sensitive to incidence angles. For a fair comparison of these configurations, we introduced the parameter Rectenna Topology Indicator (RTI). The RTI function is defined as the ratio of final available dc power from these two topologies. For $\mathrm{RTI} > 1$, the RF-combiner performs better than the DC-combiner. The converse is true for $\mathrm{RTI} < 1$. Our study showed that the RTI is affected by the following.

- N, the number of antennas in the array. An increase in N will extend the region where DC-combiner performs better.
- η, RF-to-dc conversion efficiency of the rectifier circuit as a function of input RF power. Rectifiers that exhibit convex η will extend the region where RF-combiner performs better.

The method presented in this letter can be utilized to find out which configuration will perform best without actually building and testing the rectenna arrays. Future work will focus on incorporating polarization effects within the model and conducting measurements in more realistic environments.

References

[1] R. Want, "An introduction to RFID technology," *Pervasive Comput.*, vol. 5, no. 1, pp. 25–33, Jan.–Mar. 2006.
[2] G.-R. Duncan, "Nokia developing phone that recharges itself without mains electricity," 2009 [Online]. Available: http://www.guardian.co.uk/environment/2009/jun/10/nokia-mobile-phone
[3] T. East, "A self-steering array for the SHARP microwave-powered aircraft," *IEEE Trans. Antennas Propag.*, vol. 40, no. 12, pp. 1565–1567, Dec. 1992.
[4] J. Zbitou, M. Latrach, and S. Toutain, "Hybrid rectenna and monolithic integrated zero-bias microwave rectifier," *IEEE Trans. Microw. Theory Tech.*, vol. 54, no. 1, pp. 147–152, Jan. 2006.
[5] J. Hagerty, F. Helmbrecht, W. McCalpin, R. Zane, and Z. Popovic, "Recycling ambient microwave energy with broad-band rectenna arrays," *IEEE Trans. Microw. Theory Tech.*, vol. 52, no. 3, pp. 1014–1024, Mar. 2004.
[6] N. Shinohara and H. Matsumoto, "Dependence of dc output of a rectenna array on the method of interconnection of its array elements," *Elect. Eng. Jpn.*, vol. 125, no. 1, pp. 9–17, 1998.
[7] J.-P. Curty, N. Joehl, F. Krummenacher, C. Dehollain, and M. Declercq, "A model for μ-power rectifier analysis and design," *IEEE Trans. Circuits Syst. I, Reg. Papers*, vol. 52, no. 12, pp. 2771–2779, Dec. 2005.
[8] U. Olgun, C.-C. Chen, and J. Volakis, "Low-profile planar rectenna for batteryless RFID sensors," in *Proc. APSURSI*, 2010, pp. 1–4.
[9] J. L. Volakis, C.-C. Chen, and K. Fujimoto, *Small Antennas: Miniaturization Techniques and Applications*, 1st ed. New York: McGraw-Hill, 2010.